How to cite: *Angew. Chem. Int. Ed.* **2024**, *63*, e202410169
doi.org/10.1002/anie.202410169

Photoresponsive Drugs

A Photocaged Microtubule-Stabilising Epothilone Allows Spatiotemporal Control of Cytoskeletal Dynamics

*Carina Schmitt, Philipp Mauker[+], Nynke A. Vepřek[+], Carolin Gierse, Joyce C. M. Meiring, Jürgen Kuch, Anna Akhmanova, Leif Dehmelt, and Oliver Thorn-Seshold**

Abstract: The cytoskeleton is essential for spatial and temporal organisation of a wide range of cellular and tissue-level processes, such as proliferation, signalling, cargo transport, migration, morphogenesis, and neuronal development. Cytoskeleton research aims to study these processes by imaging, or by locally manipulating, the dynamics and organisation of cytoskeletal proteins with high spatiotemporal resolution: which matches the capabilities of optical methods. To date, no photoresponsive microtubule-stabilising tool has united all the features needed for a practical high-precision reagent: a low potency and biochemically stable non-illuminated state; then an efficient, rapid, and clean photoresponse that generates a high potency illuminated state; plus good solubility at suitable working concentrations; and efficient synthetic access. We now present **CouEpo**, a photocaged epothilone microtubule-stabilising reagent that combines these needs. Its potency increases approximately 100-fold upon irradiation by violet/blue light to reach low-nanomolar values, allowing efficient photocontrol of microtubule dynamics in live cells, and even the generation of cellular asymmetries in microtubule architecture and cell dynamics. **CouEpo** is thus a high-performance tool compound that can support high-precision research into many microtubule-associated processes, from biophysics to transport, cell motility, and neuronal physiology.

Introduction

Life relies on the precise organisation of complex cellular processes. The cytoskeleton is the major player that provides spatially and temporally specific support for a myriad of processes, like intracellular transport, cell proliferation, cell motility, and neuronal development.[1–4] Microtubules (MTs) are one of the three main cytoskeletal filaments. The many hundreds of MT-dependent processes often rely on the relative stability and dynamics of MT structures. This is perhaps most clearly seen in the drastic MT reorganisations needed for spindle formation during cell division, which render MTs a prime target for antimitotic drugs.[5] Indeed, many MT-destabilising and MT-stabilising compounds (vinca alkaloids, maytansines, taxanes, epothilones) have been developed for cancer therapy.[6] As MTs are highly conserved, such small molecule drugs are also easily applicable across eukaryotic cell biology as tool compounds for cytoskeleton research. However, since so many different processes depend on MT architecture and dynamics, but all are modified at the same time by drug application, their practical utility for resolving MT-dependent biology is limited since they lack any *spatiotemporal precision of action.*

Photopharmacology aims to develop photoresponsive drugs for just such spatiotemporally resolved studies. Photoresponse can be implemented with photoswitches, or photocages (photoremovable protecting groups; irreversible uncaging).[7] MT *destabiliser* drugs can be structurally simple and easy to modify; so many photocaged,[8–10] and irreversibly[9–12] or reversibly[13–21] photoswitchable MT destabilisers have been created. These have helped uncover some spatiotemporal roles for MT-dependent processes in embryology, migration, and neuroscience.[22–28] Yet, the photopharmacology of the structurally more complex MT *stabilisers* remains poorly developed. This is problematic since stabilisation is a distinct mode of action, that is crucial to the proper study of most MT-dependent processes since these typically rely on the presence and function of MTs (whereas, chemical or optogenetic[29–32] destabilisers remove them).

Two classes of photoswitchable MT stabilisers were reported, based on taxanes (**AzTax**[33]) and epothilones

[*] C. Schmitt, P. Mauker,[+] Dr. N. A. Vepřek,[+] J. Kuch, Dr. O. Thorn-Seshold
Department of Pharmacy
Ludwig-Maximilians University of Munich
Butenandtstrasse 7, Munich 81377 (Germany)
E-mail: oliver.thorn-seshold@cup.lmu.de

C. Gierse, Dr. L. Dehmelt
Department of Chemistry and Chemical Biology
Technical University Dortmund
Otto-Hahn-Str. 4a, Dortmund 44227 (Germany)

Dr. J. C. M. Meiring, Prof. Dr. A. Akhmanova
Cell Biology, Neurobiology and Biophysics, Department of Biology
Utrecht University
Padualaan 8, 3584 CH, Utrecht (Netherlands)

[+] N.A.V. and P.M. declare equal authorships, with the right to present their author positions in either order.

(**STEpo**[34]), that allow spatiotemporal control of MT dynamics in live cells (Figure 1b). However, their light-induced increase of bioactivity was at best 6-fold (from dark to lit). This is such a narrow working window that they were only successful in cell culture (uniform concentrations), not *in vivo* (inhomogeneous concentrations). They also suffered a 20-to-100-fold loss in potency versus the parent drugs, which is unsurprising due to the steric bulk of the photoswitches. Both aspects limit their practical utility. For the epothilone **STEpo**, off-photoisomerisation was not possible since the heterostilbene can only be effectively switched to a *Z*-isomer-enriched photostationary state (PSS), not switched back to an *E*-rich PSS; but it was also found that the bioactivity of the taxane **AzTax3MP** was not efficiently "photoreversible" even by active bidirectional photoswitching in cells, and rather was accomplished by diffusion. Together, these features encouraged us to now explore either photoreversible epothilone switches (unknown), or else to accept diffusion-based reversibility and work instead on improving the performance of photocaged MT-stabilisers.

No photocaged epothilones have been reported. Several photocaged taxanes have been developed (Figure 1a), but they are not widely used: they suffer inefficient and unclean photouncaging, mostly needing UV light (*ortho*-nitrobenzyl, coumarin, amino-1,4-benzoquinone cages);[36] their solubility at working concentrations is famously poor;[37] and most reagents either masked the $O^{2'}$ and/or O^{7} hydroxyls as potentially biochemically unstable carbonates,[36,38,39] or else the $N^{3'}$ amine which does not offer a large activity turn-on upon unmasking.[37,39] In fact, although the "photo-turn-on of activity" is a major determinant of how useful a caged tool can be, the degree of turn-on was not even reported for many of them.[37,39] Also, as del Campo showed, properly silencing taxane bioactivity by hydroxyl photocaging requires *both* C2′ and C7 alcohols to be masked:[36] squaring the problems of photouncaging. Indeed, the only commercial caged stabiliser (Molecular Probes **caged taxol**) was discontinued 20 years ago, likely due to these problems.[36]

Therefore, we considered that no available photoresponsive reagent features the required combination of a biochemically stable low-potency non-illuminated state, with efficient and clean photoresponse, giving a high-potency illuminated state, where the reagent has efficient synthesis and good solubility at the working concentration. To address this unmet need, we aimed to develop novel derivatives of MT-stabilisers ZK-Epothilone (**ZK-Epo**) and paclitaxel. Our pursuit of reversibly photoswitchable azobenzene epothilones (**AzoEpo**) was stymied by synthetic roadblocks, and our visible-light-uncaged paclitaxels (**CouTax**) had poor potency in the lit state. However, we obtained the first photouncageable epothilone (**CouEpo**), which has low/mid-nanomolar bioactivity after photouncaging by visible light, with 100-fold lower bioactivity before uncaging, making it a practical tool that has succeeded in reproducible, efficient, live cell photocontrol of MT dynamics and associated downstream processes.

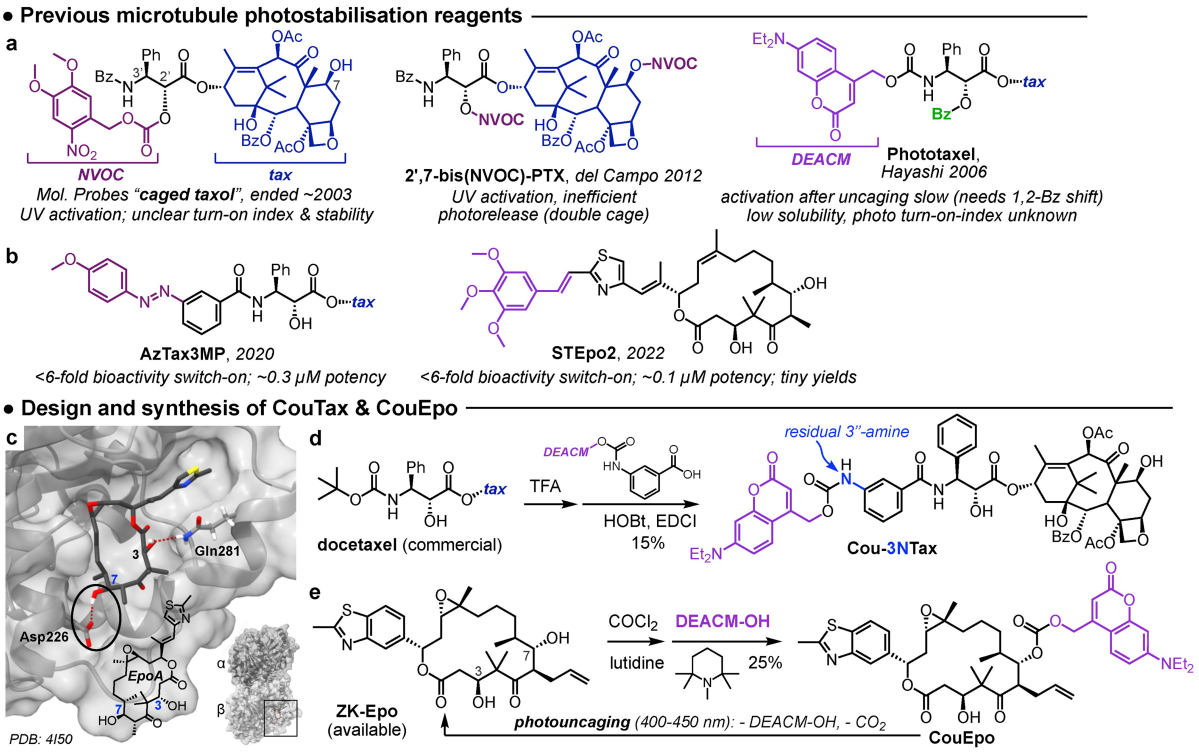

Figure 1. Prior Art, Design, and Synthesis. a,b) Prior art photoresponsive chemical tools for MT photostabilisation. c) Published epothilone A: tubulin structure (PDB 4I50),[35] with H-bonds to Gln281 and Asp226 in red. d) Synthesis of **Cou-3NTax** from docetaxel. e) Synthesis and photouncaging of **CouEpo**. *See Figure S9 for high-resolution vectorial image.*

Results and Discussion

Initial Approach: Novel Caged Taxanes

Initially, we aimed to develop photocaged derivatives of the chemically more tractable taxanes, particularly to overcome the limited temporal resolution that prior art reagents suffered due to their slow release (**Phototaxel** needs an extra 1,2-benzoyl shift to give bioactivity) or need for double uncaging (**2′,7-bis(NVOC)-PTX**). Our idea was to instead cage an unnatural aniline nitrogen in *meta* or *para* on the sidechain 3′-benzamide, since SAR studies led us to expect this amine should be tolerated, and since the cage could then be applied as a biochemically stable carbamate. We chose a photon-efficient diethylaminocoumarin cage (DEACM; 400–450 nm),[40] which gave designs **Cou-3NTax** (Figure 1d) and **Cou-4NTax** (Figure S1). However, the free anilines' potencies were ca. 60-fold lower (EC_{50}~0.2 μM) than paclitaxel; so although the DEACM carbamates of **3NTax** and **4NTax** could be efficiently and cleanly uncaged with >50 % yield (Figure S2), we expected their practical utility would be limited. Indeed, while photouncaging **Cou-3NTax** gave a substantial potency increase (35-fold EC_{50} change: from 30 μM dark to 0.84 μM uncaged, Figure S2d), and while it successfully photoinduced MT stabilisation in acute live cell imaging assays (Figure S3, Movie S3), the high-μM concentrations needed for efficient cell work with these low-potency cores made us fear solubility and reproducibility problems in more meaningful, more complex systems (Supporting Note 1). Since epothilones have greater potency and more reliable solubility than taxanes, we focused on them instead for *practical* MT-stabiliser photopharmaceuticals.

Failed Attempt: Reversibly Photoswitchable Epothilone

We previously reported **STEpo** epothilones designed to use a stilbene photoswitch to light-dependently control bioactivity, by *Z*-isomer-dependently forming a key hydrogen bond (from the thiazole nitrogen to Thr274 on tubulin, which stabilises the M-loop that in turn makes a lateral contact stabilising the MT lattice).[35] Those **STEpo**s were accessed in low yield by Horner–Wadsworth–Emmons (HWE) olefinations of a synthetically accessible epothilone methyl ketone.[41] Now, we intended to attach thiazolo-azobenzene photoswitches to the epothilone instead, to achieve **AzoEpo** reagents that should be bidirectionally photoswitchable between *Z*- and *E*-rich PSSs. Although thiazolo-azobenzenes underwent smooth HWE, Wittig and Julia-Kociensky olefinations with model aldehydes, only decomposition products resulted from reactions with ketones including the target epothilone methyl ketone. Poor to zero yields were likewise obtained for olefin metathesis reactions between thiazolo azobenzenes and model substrates (Figures S4 and S5 and Supporting Note 2), leading us to abandon this approach once the success of the epothilone photocaging strategy became apparent.

Final Approach: Synthesis of Caged Epothilone CouEpo

We chose **ZK-Epo** for photocaging, for its high potency (< 1 nM), good solubility at this concentration, and since it efficiently enters cells and evades efflux pumps.[42] Considering published cryo-EM epothilone A:tubulin structures,[35] we aimed to introduce a photocage to block binding or mask interactions that are key for bioactivity (Figure 1c). Four hydrogen bonds are formed in the structure. Those from the C3 and C7 hydroxyls (to Gln281 and Asp226 of β-tubulin)[35] seemed promising, since caging them should impair binding affinity both by preventing H-bond donation, and due to steric pressure from the DEACM cage.

Alcohol functionalities are usually photocaged with photoremovable protecting groups as carbonates.[40] The **ZK-Epo** secondary alcohols at C3 and C7 were very inert, and did not react with *para*-nitrophenylchloroformate, carbonyldiimidazole, bis(pentafluorophenyl) carbonate, or even triphosgene under usual conditions. However, phosgene in toluene gave the C7 chloroformate exclusively; with an excess of the sterically hindered base 1,2,2,6,6-pentamethylpiperidine, that avoids elimination of the chloroformate, this could be coupled to DEACM-OH to give C7-caged **CouEpo** in decent yield (25 %, Figure 1e).

Photochemical Properties and GFP-Orthogonality

The photouncaging response of **CouEpo** is ca. 15 nm red-shifted[43] from its absorption spectrum, peaking at 405–435 nm (Figure 2a), though uncaging is effective from 385–460 nm. Thus, **CouEpo** can be uncaged by the common microscopy lasers at 405 and 440 nm, avoiding the damaging UV light that e.g. *ortho*-nitrobenzyl cages require. Also, it is almost unaffected by typical GFP/YFP excitation (490/514 nm), which is practical for biology since cytoskeleton studies often use multichannel imaging. Crucially, photouncaging was clean: the only products detectable in HPLC were active **ZK-Epo** and DEACM-OH (Figure 2b,c; and DEACM-OH was negligibly toxic or phototoxic compared to **ZK-Epo**: see Figure S6). The **ZK-Epo** photo-yield of ~50 % fits previous coumarin reports.[37]

CouEpo Gives Photocontrolled Bioactivity in Live Cells

MT stabilisation inhibits cell proliferation by blocking mitosis. Since proliferation is easy to screen, we first tested the cellular utility of **CouEpo** by long-term assays of light-and-concentration-dependent antiproliferative activity (Figure 2d). This can test for undesired complications, like non-photolytic uncaging (e.g., hydrolysis in the dark), or phototoxicity (e.g., if apparent toxicity for lit **CouEpo** would be higher than reference **ZK-Epo**). However, **CouEpo** matched expectations for an ideal photocaged drug. In the dark (EC_{50} > 94 nM), **CouEpo** was ~100-fold less potent than its parent **ZK-Epo** (EC_{50} < 1 nM), showing excellent bioactivity blocking and biochemical stability of the cage. Brief *in situ* illumination with low-intensity LEDs at 400–435 nm,[13]

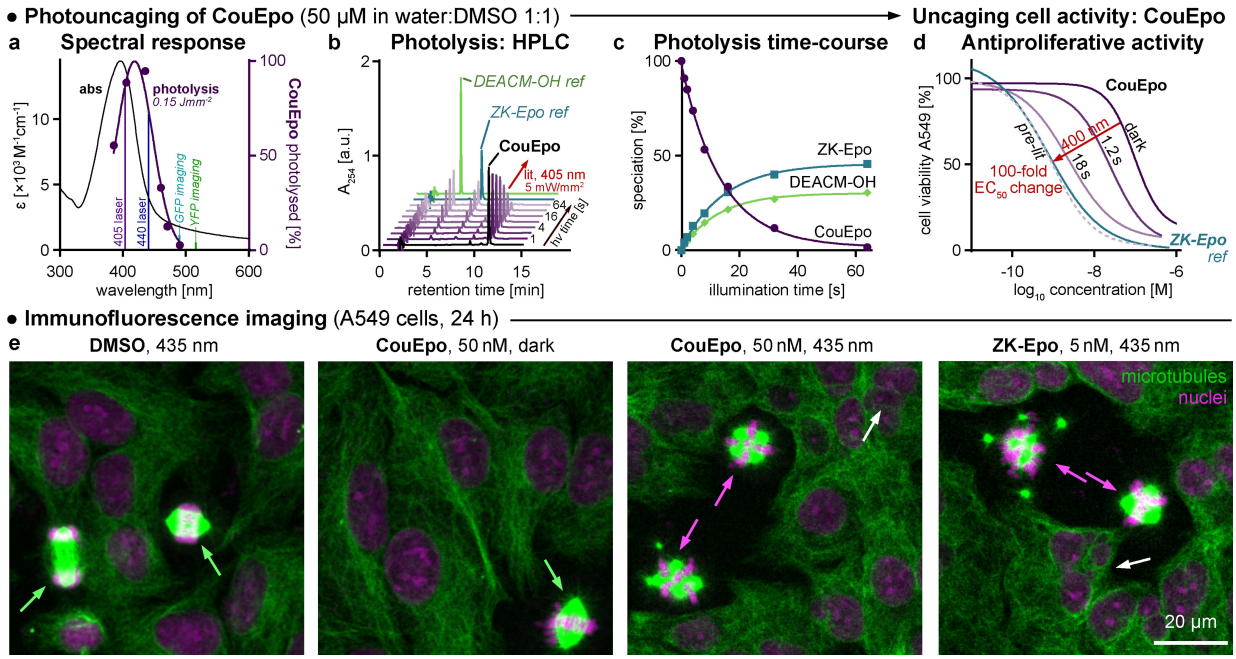

Figure 2. Photochemistry and cell activity of **CouEpo**. a) Absorptivity versus photochemical reactivity. b,c) HPLC speciation of **CouEpo** photolysis (time-course). d) **CouEpo** has potent, light-dependent antiproliferative activity, with EC_{50}s: dark: 94 nM; 1.2 s illumination: 25 nM, 18 s illumination: 2.4 nM; pre-UV-illuminated (*ex situ*): 0.9 nM; vs reference **ZK-Epo**: 0.8 nM (light: 400 nm, as 100 ms pulses every 10 s; A549 cells, 48 h, three replicates, shown as means). e) Confocal images (63×) of A549 cells treated for 24 h under lit (36 s, 435 nm) or dark conditions. Green arrows: normally dividing cells (bipolar), magenta arrows: irregular mitotic spindles (tripolar / tetrapolar), white arrows: multinucleated cells. (Nuclei in magenta (propidium iodide), MTs in green (anti-α-tubulin-FITC), scale bar 20 µm; expanded fields of view shown in Figure S6). *See Figure S10 for high-resolution vectorial image.*

returned low nanomolar potency nearly identical to that of **ZK-Epo** or *ex situ* pre-lit **CouEpo** stocks (Figure 2d), while illumination at 490 nm had no effect relative to dark conditions (Figure S6). These results align with the spectral response shown in cell-free assays (Figure 2a), affirming that **CouEpo** can be operated with typical photoactivation laser wavelengths and yet is orthogonal to typical imaging wavelengths (details in Supporting Note 3.1).

To support that the mechanism of action from **CouEpo** uncaging is MT inhibition, we examined MT architecture and cell status before and after irradiation. A549 cells treated with **CouEpo** (50 nM) in the dark were similar to DMSO-only controls: cells were mononuclear, with regular MT architectures, and some regular bipolar mitotic figures (green arrows, Figure 2e). Pulsing **CouEpo** at 435 nm (100 ms every 10 s, for 1 h at treatment start) disorganised the MT architectures; multinuclear cells were common (faulty mitosis; white arrows); and faulty tri- or tetrapolar mitotic figures were strikingly common (magenta arrows; Figure 2e; full data in Figure S6). This further supports that **CouEpo** light-dependently inhibits MT dynamics and architecture.

Time-Resolved Photocontrol of MT Dynamics

MT polymerisation dynamics can be tracked with fluorescently marked End-Binding protein EB3, which visualises growing MT tips as "comets".[44] MT stabilisers suppress normal MT remodelling rates by locking tubulin into polymerised MTs, so bioactive compounds reduce the number of EB3 "comets" as well as their velocity.[13,45] To test if uncaging **CouEpo** disrupts live cell MT dynamics with temporal specificity, we first imaged EB3-3×mScarlet-I expressing A549 cells treated with **CouEpo** (150 nM). EB3 comet counts dropped greatly upon uncaging by full field of view (FOV) laser scanning illumination at 405 nm (Figure 3, Movie S1). To proceed towards spatial specificity, we next tested localised 405 nm photoactivation in a sub-region of the FOV, taking advantage of the GFP orthogonality of **CouEpo** to image EB3-GFP in HeLa cells. A full discussion of the results is given at Supporting Note 3.2; in brief, **CouEpo** (75 nM) did not affect EB3 comet density and velocity during GFP imaging, but pulsing at 405 nm even just outside the cells of interest steadily decreased the density, velocity, and size of EB3 comets (Figure S7c–f, Movies S4 and S5), without recovery during subsequent imaging. Thus, irreversible uncaging of **CouEpo** suppresses MT dynamics in live cells with temporal precision.

Spatiotemporally Resolved MT Photocontrol

We then set out to probe the spatiotemporal precision of MT control that can be attained within cells in practical conditions, under subcellularly localised photoactivation protocols. GFP-tubulin expressing PtK1 (potoroo kidney) cells, treated with **CouEpo** (100 nM), were locally illumi-

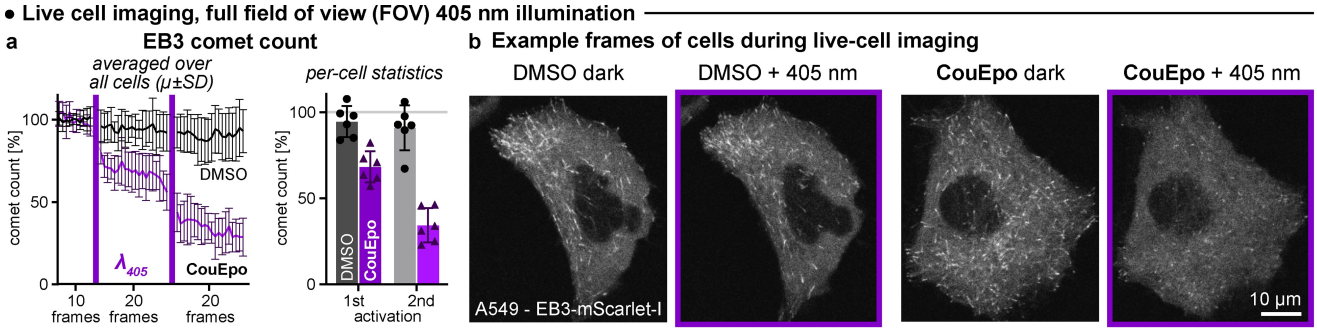

Figure 3. Photocontrol of MT dynamics with **CouEpo**. a) Normalised EB3 comet counts in **CouEpo** or DMSO-only treated cells, either averaged over all cells, or given per cell ($n = 6$ cells each) after 1 or 2 full FOV 405 nm photoactivations. b) Cell images before/after two 405 nm applications (time-courses: Movies S1 and S2; see also Figure S7; scale bar is 10 μm). *See Figure S11 for high-resolution vectorial image with expanded legend.*

nated with 405 nm near a cell edge, at a diffraction-limited photoactivation spot (indicated on images with a purple circle) applied once every 100 s by a standard FRAP module, during ongoing TIRF imaging at 514 nm (Figure 4). Since TIRF images $\lesssim 250$ nm of cell thickness next to the coverslip, this reveals the segments of microtubules that enter the imaging slice, rather than long MT filaments.

To assess the subcellular localisation of cell effects, we used the position of the photoactivation spot relative to the cell centroid to define a "front" region at the proximal cell edge and compared it to the "back" region at the opposite cell edge (Figure 4b). MT stabilisation increases the amount of tubulin incorporated into MT polymer, which should increase the GFP reporter signal. Indeed, photoactivation induced a strongly localised change in tubulin distribution, enriching the signal in the front of the cell without affecting the back (Figure 4c,d).

Furthermore, MTs can promote cell protrusion, via their mechanical properties as well as their roles in intracellular trafficking and signalling.[3,25,26] Thus, local MT stabilisation should lead to increased local protrusion of the cell edge. We analysed local cell protrusion within a region of interest (ROI) centred on the photoactivation spot, by quantifying the change in cell area coverage of this ROI after 405 nm

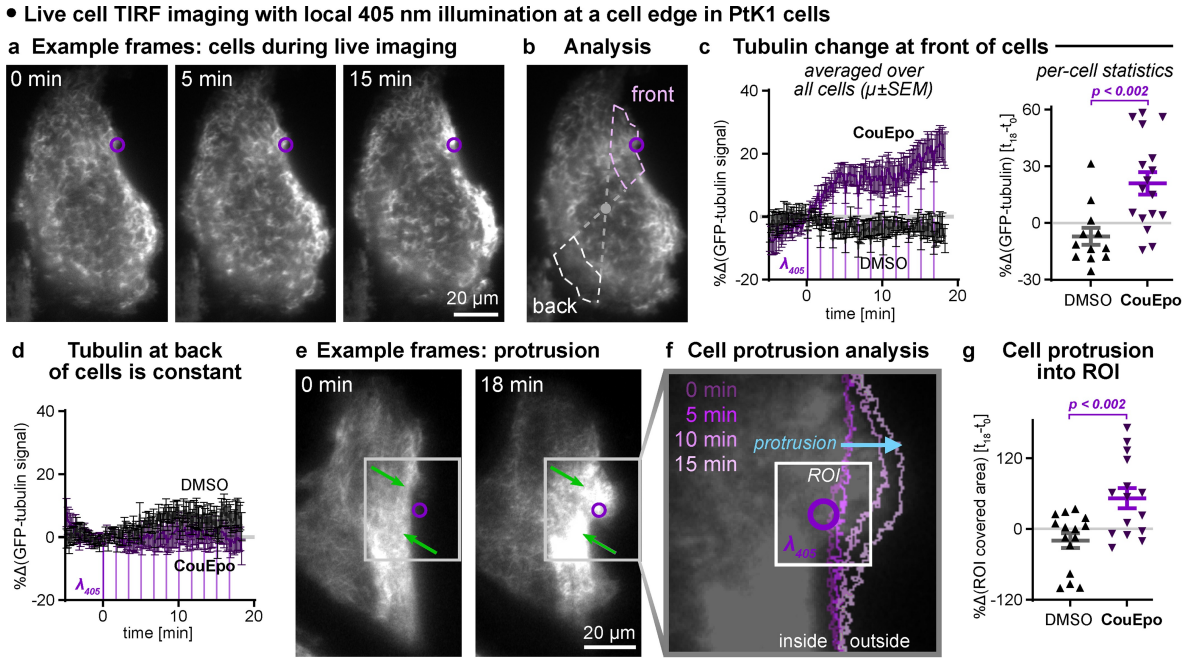

Figure 4. Subcellular photocontrol of tubulin dynamics by local 405 nm spot photoactivation in PtK1 cells expressing GFP-tubulin, treated with 100 nM **CouEpo** or DMSO cosolvent only, imaged by TIRF microscopy (photoactivation at purple circle starts at 0 min). a–d) Cell images, analysis, and quantification of GFP-tubulin signal intensity at the front (cell edge near the photoactivation site) or back (the opposite cell edge). e–g) Cell images, analysis, and quantification of cell area coverage within a ROI centred on the photoactivation spot. Panel **f** shows a zoom on the grey boxed region from panel **e**, with coloured lines indicating the cell border over time during photoactivation, and the white boxed ROI that was used to quantify protrusion. All scale bars 20 μm; "%Δ" indicates percent change relative to the value at time 0 (alternative data representations shown in Figure S8; one cell per datapoint in panels **c**,**g**). *See Figure S12 for high-resolution vectorial image with expanded legend.*

photoactivation (Figure 4e,f). Coverage was considerably increased after illumination (Figure 4g, Figure S8). DMSO-only controls showed no increase of local tubulin signal or of ROI coverage (Figure 4c,d,g). Taken together, these data show precise targeted remodelling of the MT cytoskeleton with associated effects on cellular function, using simple FRAP-targeted photoactivation of **CouEpo** orthogonal to ongoing imaging, with commonlaser lines.

Conclusion

We introduce an optically controlled MT-modulator that we argue is the first reagent that can combine highly effective, practical, and robust MT photostabilisation. **CouEpo** is the first photocaged epothilone; it is efficiently photoactivated by UV, violet and blue light (360–460 nm, including the 405 and 440 nm lasers that are common in microscopy); it gives a ~100-fold bioactivity increase upon uncaging of its single cage group; and when uncaged it reaches ca. 1 nM potency (allowing low working concentrations, that avoid solubility issues, to be effective). Its cage resists cleavage by wavelengths $\geq$ 490 nm, making it compatible with imaging fluorophores in all common channels (GFP, YFP, RFP), and its caged form is biochemically stable in cells in the long term. It is by virtue of this *combination* of features that we feel **CouEpo** substantially improves over all previous photopharmaceutical MT stabilisers, whether photouncaged or photoswitchable. **CouEpo** has shown high spatial and temporal precision control over MT stabilisation, in settings from whole-cell activation (Figure 3a,b) down to asymmetric effects within single cells (Figure 4), and is now ready for wider applications in biology.

Epothilones are produced on the multikilogram scale for cancer therapy in the clinic or in clinical trials; and the C7′ alcohol is conserved in all of them. We expect that the simplicity of the conditions we show for transforming **ZK-Epo** (brand name Sagopilone) into C7′-photocaged **CouEpo** will easily translate to the other common epothilones (epothilones A-D/Patupilone and Utidelone; azaepothilone/Ixabepilone; etc) to allow any available epothilone to be caged, as well as to allow different cages to be used if it is desirable to tune spectral response or uncaging yields (although we consider that the DEACM cage already occupies the most useful spectral window for cell biology use, and it does not seem to cause biodistribution or phototoxicity complications). Thus, while we are freely distributing our stocks of **CouEpo** for cell biology research upon reasonable request, we expect that such reagents will be readily synthesisable in many groups, and if they would one day be distributed, it would fill the current gap in the reagent toolbox for effective MT photostabiliser reagents. We expect this relative ease of access will couple with the practicality and power of such reagents, as we demonstrate here in cell culture, to encourage their wider adoption as high-precision tools: for cytoskeleton biophysics; for cell motility, division, and intracellular transport studies in chemical and cell biology; and ultimately for developmental and *in vivo* studies.

Supporting Information

(1) Movies S1 and S2 corresponding to Figure 3 (AVI), Movie S3 corresponding to Figure S3 (AVI), Movies S4 and S5 corresponding to Figure S7 (MP4), Movies S6 and S7 corresponding to Figure 4 (AVI). (2) Supporting Note 1 (design and performance of **CouTax** reagents); Supporting Note 2 (attempted **AzoEpo** syntheses); Supporting Note 3 (additional data for **CouEpo**); and all compound synthesis, analysis, and biological applications (PDF). The authors have cited additional references within the Supporting Information.[46–57]

Abbreviations

DEACM-OH	7-(diethylamino)coumarin-4-methanol
EB3	microtubule plus end-binding protein 3
FRAP	fluorescence recovery after photobleaching module
GFP	green fluorescent protein (typ. ex. 488 nm, 514 nm also feasible)
MT	microtubule
PSS	photostationary state
RFP	red fluorescent protein (typ. ex. 561 nm)
TIRF	total internal reflection fluorescence microscopy
YFP	yellow fluorescent protein (typ. ex. 514 nm)

Author Contributions

C.S. performed synthesis, photocharacterisation, data collection, figure preparation, some photocontrol studies, and first draft writing, concerning **CouEpo** and **AzoEpo** (all relevant Figures incl. Figures 2a–d, S4, S5, S6a). P.M. performed synthesis, photocharacterisation, data collection, figure preparation, and first draft writing, concerning **CouTax** (Figures S1–S3), and supervised J.K. to perform synthesis. N.A.V. performed fixed and live A549 cell studies including cell imaging and photocontrol, statistical analysis, and first draft writing (Figures 2d,e, 3, S3, S6, S7ab, and Movies S1–S3). L.D. performed and supervised C.G. to perform PtK1 cell imaging and photocontrol studies, and statistical analysis (Figures 4, S6 and Movies S6 and S7). J.C.M.M. performed HeLa cell imaging and photocontrol studies, statistical analysis, and figure preparation, as supervised by A.A. (Figure S5c–f and Movies S4 and S5). O.T.-S. conceived and supervised the study and wrote the manuscript with input from all authors.

Acknowledgements

This research was supported by funds from the German Research Foundation (DFG: SPP 1926 project number 426018126 to L.D. and O.T.-S.; Emmy Noether grant number 400324123, SFB 1032 project B09 number

201269156, and SFB TRR 152 project P24 number 239283807 to O.T.-S.; Heisenberg Programme Grant 823/8-1 and Principal Investigator grant 823/10-1 to L.D.) and the Netherlands Organization for Scientific Research (NWO: Gravitation programme IMAGINE! project number 24.005.009 to A.A.). C.S. and P.M. acknowledge financial support from Studienstiftung d.d.V. PhD scholarships. P.M. acknowledges support from a Joachim Herz Foundation Add-on Fellowship. J.C.M.M. acknowledges support from an EMBO Long Term Fellowship (ALTF 261-2019). We thank Jan Huebner (Bayer) for the gift of **ZK-Epo** that was arranged through the goodwill of Dirk Trauner (NYU). We thank Anja Biesemann (TU Dortmund) who generated the PtK1 cell line stably expressing GFP-tubulin. Open Access funding enabled and organized by Projekt DEAL.

Conflict of Interest

The authors declare no conflict of interest.

Data Availability Statement

The data that support the findings of this study are available in the supplementary material of this article.

Keywords: Epothilones · Microtubule Stabilisers · Natural Products · Photopharmacology · Photocaging

[1] S. Forth, T. M. Kapoor, *J. Cell Biol.* **2017**, *216*, 1525–1531.
[2] M. Burute, L. C. Kapitein, *Annu. Rev. Cell Dev. Biol.* **2019**, *35*, 29–54.
[3] S. Etienne-Manneville, *Annu. Rev. Cell Dev. Biol.* **2013**, *29*, 471–499.
[4] L. C. Kapitein, C. C. Hoogenraad, *Neuron* **2015**, *87*, 492–506.
[5] C. Dumontet, M. A. Jordan, *Nat. Rev. Drug Discovery* **2010**, *9*, 790–803.
[6] J. R. Peterson, T. J. Mitchison, *Chem. Biol.* **2002**, *9*, 1275–1285.
[7] K. Hüll, J. Morstein, D. Trauner, *Chem. Rev.* **2018**, *118*, 10710–10747.
[8] M. Wühr, E. S. Tan, S. K. Parker, H. W. Detrich, T. J. Mitchison, *Curr. Biol.* **2010**, *20*, 2040–2045.
[9] R. Bisby, S. Botchway, J. Hadfield, A. McGown, K. M. Scherer, *Multi-Photon Isomerisation Of Combretastatins And Their Use In Therapy* **2013**, WO2013021208.
[10] J. Hadfield, A. McGown, S. Mayalarp, E. Land, I. Hamblett, K. Gaukroger, N. Lawrence, L. Hepworth, J. Butler, *Substituted Stilbenes, Their Reactions And Anticancer Activity* **2002**, WO200250007.
[11] L. Gao, J. C. M. Meiring, Y. Kraus, M. Wranik, T. Weinert, S. D. Pritzl, R. Bingham, E. Ntouliou, K. I. Jansen, N. Olieric, J. Standfuss, L. C. Kapitein, T. Lohmüller, J. Ahlfeld, A. Akhmanova, M. O. Steinmetz, O. Thorn-Seshold, *Cell Chem. Biol.* **2021**, *28*, 228–241.e6.
[12] L. Gao, J. C. M. Meiring, A. Varady, I. E. Ruider, C. Heise, M. Wranik, C. D. Velasco, J. A. Taylor, B. Terni, T. Weinert, J. Standfuss, C. C. Cabernard, A. Llobet, M. O. Steinmetz, A. R. Bausch, M. Distel, J. Thorn-Seshold, A. Akhmanova, O. Thorn-Seshold, *J. Am. Chem. Soc.* **2022**, *144*, 5614–5628.
[13] M. Borowiak, W. Nahaboo, M. Reynders, K. Nekolla, P. Jalinot, J. Hasserodt, M. Rehberg, M. Delattre, S. Zahler, A. Vollmar, D. Trauner, O. Thorn-Seshold, *Cell* **2015**, *162*, 403–411.
[14] A. J. Engdahl, E. A. Torres, S. E. Lock, T. B. Engdahl, P. S. Mertz, C. N. Streu, *Org. Lett.* **2015**, *17*, 4546–4549.
[15] S. K. Rastogi, Z. Zhao, S. L. Barrett, S. D. Shelton, M. Zafferani, H. E. Anderson, M. O. Blumenthal, L. R. Jones, L. Wang, X. Li, C. N. Streu, L. Du, W. J. Brittain, *Eur. J. Med. Chem.* **2018**, *143*, 1–7.
[16] A. Sailer, F. Ermer, Y. Kraus, F. Lutter, C. Donau, M. Bremerich, J. Ahlfeld, O. Thorn-Seshold, *ChemBioChem* **2019**, *20*, 1305–1314.
[17] A. Sailer, F. Ermer, Y. Kraus, R. Bingham, F. H. Lutter, J. Ahlfeld, O. Thorn-Seshold, *Beilstein J. Org. Chem.* **2020**, *16*, 125–134.
[18] A. Sailer, J. C. M. Meiring, C. Heise, L. N. Pettersson, A. Akhmanova, J. Thorn-Seshold, O. Thorn-Seshold, *Angew. Chem. Int. Ed.* **2021**, *60*, 23695–23704.
[19] J. E. Sheldon, M. M. Dcona, C. E. Lyons, J. C. Hackett, M. C. T. Hartman, *Org. Biomol. Chem.* **2016**, *14*, 40–49.
[20] S. Kirchner, A.-L. Leistner, P. Gödtel, A. Seliwjorstow, S. Weber, J. Karcher, M. Nieger, Z. Pianowski, *Nat. Commun.* **2022**, *13*, 6066.
[21] A. Seliwjorstow, M. Takamiya, S. Rastegar, Z. Pianowski, *ChemBioChem* **2024**, e202400143.
[22] J. Zenker, M. D. White, R. M. Templin, R. G. Parton, O. Thorn-Seshold, S. Bissiere, N. Plachta, *Science* **2017**, *357*, 925–928.
[23] A. Singh, T. Saha, I. Begemann, A. Ricker, H. Nüsse, O. Thorn-Seshold, J. Klingauf, M. Galic, M. Matis, *Nat. Cell Biol.* **2018**, *20*, 1126–1133.
[24] C. Vandestadt, G. C. Vanwalleghem, M. A. Khabooshan, A. M. Douek, H. A. Castillo, M. Li, K. Schulze, E. Don, S.-A. Stamatis, M. Ratnadiwakara, M.-L. Änkö, E. K. Scott, J. Kaslin, *Dev. Cell* **2021**, *56*, 2364–2380.e8.
[25] A. Kopf, J. Renkawitz, R. Hauschild, I. Girkontaite, K. Tedford, J. Merrin, O. Thorn-Seshold, D. Trauner, H. Häcker, K.-D. Fischer, E. Kiermaier, M. Sixt, *J. Cell Biol.* **2020**, *219*, e201907154.
[26] U. Theisen, A. U. Ernst, R. L. S. Heyne, T. P. Ring, O. Thorn-Seshold, R. W. Köster, *J. Cell Biol.* **2020**, *219*, e201908040.
[27] C. Nakajima, M. Sawada, E. Umeda, Y. Takagi, N. Nakashima, K. Kuboyama, N. Kaneko, S. Yamamoto, H. Nakamura, N. Shimada, K. Nakamura, K. Matsuno, S. Uesugi, N. A. Vepřek, F. Küllmer, V. Nasufović, H. Uchiyama, M. Nakada, Y. Otsuka, Y. Ito, V. Herranz-Pérez, J. M. García-Verdugo, N. Ohno, H.-D. Arndt, D. Trauner, Y. Tabata, M. Igarashi, K. Sawamoto, *Nat. Commun.* **2024**, *15*, 1877.
[28] K. Eguchi, Z. Taoufiq, O. Thorn-Seshold, D. Trauner, M. Hasegawa, T. Takahashi, *J. Neurosci.* **2017**, *37*, 6043–6052.
[29] J. Van Haren, R. A. Charafeddine, A. Ettinger, H. Wang, K. M. Hahn, T. Wittmann, *Nat. Cell Biol.* **2018**, *20*, 252–261.
[30] R. C. Adikes, R. A. Hallett, B. F. Saway, B. Kuhlman, K. C. Slep, *J. Cell Biol.* **2018**, *217*, 779–793.
[31] J. C. M. Meiring, I. Grigoriev, W. Nijenhuis, L. C. Kapitein, A. Akhmanova, *Curr. Biol.* **2022**, *32*, 4660–4674.e6.
[32] G. Y. Liu, S. Chen, G. Lee, K. Shaiv, P. Chen, H. Cheng, S. Hong, W. Yang, S. Huang, Y. Chang, H. Wang, C. Kao, P. Sun, M. Chao, Y. Lee, M. Tang, Y. Lin, *EMBO J.* **2022**, *41*, e110472.
[33] A. Müller-Deku, J. C. M. Meiring, K. Loy, Y. Kraus, C. Heise, R. Bingham, K. I. Jansen, X. Qu, F. Bartolini, L. C. Kapitein, A. Akhmanova, J. Ahlfeld, D. Trauner, O. Thorn-Seshold, *Nat. Commun.* **2020**, *11*, 4640.

[34] L. Gao, J. C. M. Meiring, C. Heise, A. Rai, A. Müller-Deku, A. Akhmanova, J. Thorn-Seshold, O. Thorn-Seshold, *Angew. Chem. Int. Ed.* **2022**, *61*, e202114614.
[35] A. E. Prota, K. Bargsten, D. Zurwerra, J. J. Field, J. F. Díaz, K.-H. Altmann, M. O. Steinmetz, *Science* **2013**, *339*, 587–590.
[36] R. A. Gropeanu, H. Baumann, S. Ritz, V. Mailänder, T. Surrey, A. del Campo, *PLoS One* **2012**, *7*, e43657.
[37] M. Skwarczynski, M. Noguchi, S. Hirota, Y. Sohma, T. Kimura, Y. Hayashi, Y. Kiso, *Bioorg. Med. Chem. Lett.* **2006**, *16*, 4492–4496.
[38] C.-J. Carling, J. Olejniczak, A. Foucault-Collet, G. Collet, M. L. Viger, V. A. N. Huu, B. M. Duggan, A. Almutairi, *Chem. Sci.* **2016**, *7*, 2392–2398.
[39] M. Noguchi, M. Skwarczynski, H. Prakash, S. Hirota, T. Kimura, Y. Hayashi, Y. Kiso, *Bioorg. Med. Chem.* **2008**, *16*, 5389–5397.
[40] P. Klán, T. Šolomek, C. G. Bochet, A. Blanc, R. Givens, M. Rubina, V. Popik, A. Kostikov, J. Wirz, *Chem. Rev.* **2013**, *113*, 119–191.
[41] K. C. Nicolaou, D. Rhoades, Y. Wang, R. Bai, E. Hamel, M. Aujay, J. Sandoval, J. Gavrilyuk, *J. Am. Chem. Soc.* **2017**, *139*, 7318–7334.
[42] U. Klar, B. Buchmann, W. Schwede, W. Skuballa, J. Hoffmann, R. B. Lichtner, *Angew. Chem.* **2006**, *118*, 8110–8116.
[43] I. M. Irshadeen, S. L. Walden, M. Wegener, V. X. Truong, H. Frisch, J. P. Blinco, C. Barner-Kowollik, *J. Am. Chem. Soc.* **2021**, *143*, 21113–21126.
[44] T. Stepanova, J. Slemmer, C. C. Hoogenraad, G. Lansbergen, B. Dortland, C. I. De Zeeuw, F. Grosveld, G. Van Cappellen, A. Akhmanova, N. Galjart, *J. Neurosci.* **2003**, *23*, 2655–2664.
[45] E. B. Merriam, M. Millette, D. C. Lumbard, W. Saengsawang, T. Fothergill, X. Hu, L. Ferhat, E. W. Dent, *J. Neurosci.* **2013**, *33*, 16471–16482.
[46] S. Jiang, N. Mani, E. M. Wilson-Kubalek, P.-I. Ku, R. A. Milligan, R. Subramanian, *Dev. Cell* **2019**, *49*, 711–730.e8.
[47] B. Baumgartner, V. Glembockyte, R. Mayer, A. Gonzalez-Hernandez, R. Kindler, A. Valavalkar, A. Wiegand, A. Müller-Deku, L. Grubert, F. Steiner, C. Gross, M. Reynders, V. Grenier, J. Broichhagen, S. Hecht, P. Tinnefeld, A. Ofial, B. Dietzek-Ivanšic, J. Levitz, O. Thorn-Seshold, *ChemRxiv.* **2023**, DOI 10.26434/chemrxiv-2023-37sv4.
[48] R. Lin, P. K. Hashim, S. Sahu, A. S. Amrutha, N. M. Cheruthu, S. Thazhathethil, K. Takahashi, T. Nakamura, T. Kikukawa, N. Tamaoki, *J. Am. Chem. Soc.* **2023**, *145*, 9072–9080.
[49] T. Weinrich, M. Gränz, C. Grünewald, T. F. Prisner, M. W. Göbel, *Eur. J. Org. Chem.* **2017**, *2017*, 491–496.
[50] J. L. McLaughlin, R. W. Miller, R. G. Powell, C. R. Smith, *J. Nat. Prod.* **1981**, *44*, 312–319.
[51] A. Alshargabi, G.-Y. Yeap, D. Takeuchi, M. M. Ito, *Mol. Cryst. Liq. Cryst.* **2013**, *575*, 128–139.
[52] M. Dogterom, B. Yurke, *Science* **1997**, *278*, 856–860.
[53] F. Gittes, B. Mickey, J. Nettleton, J. Howard, *J. Cell Biol.* **1993**, *120*, 923–934.
[54] L. Dehmelt, P. Nalbant, W. Steffen, S. Halpain, *Brain Cell Bio* **2007**, *35*, 39–56.
[55] N. L. Prigozhina, C. M. Waterman-Storer, *Curr. Biol.* **2004**, *14*, 88–98.
[56] B. Baumgartner, V. Glembockyte, A. Gonzalez-Hernandez, A. Valavalkar, R. Mayer, L. Fillbrook, A. Müller-Deku, J. Zhang, F. Steiner, A. Wiegand, C. Gross, M. Reynders, H. Munguba, A. Arefin, A. Ofial, J. Beves, T. Lohmüller, B. Dietzek-Ivansic, J. Broichhagen, P. Tinnefeld, J. Levitz, O. Thorn-Seshold, *ChemRxiv.* **2024**, DOI 10.26434/chemrxiv-2024-vm4n3.
[57] M. Reynders, M. Garscia, A. Müller-Deku, M. Wranik, K. Krauskopf, L. de la Osa de la Rosa, K. Schaffer, A. Jötten, A. Rode, V. Stierle, Y. Kraus, B. Baumgartner, A. Ali, A. Bubeneck, T. Seal, M. Steinmetz, P. Paulitschke, O. Thorn-Seshold, *ChemRxiv.* **2024**, DOI 10.26434/chemrxiv-2024-501qf.

Manuscript received: May 29, 2024
Accepted manuscript online: July 3, 2024
Version of record online: September 17, 2024